ACS APPLIED MATERIALS & INTERFACES

Research Article

www.acsami.org

Degradation Mechanism of Benzodithiophene-Based Conjugated Polymers when Exposed to Light in Air

Salima Alem,[†] Salem Wakim,[†] Jianping Lu,[†,*] Gilles Robertson,[‡] Jianfu Ding,[‡] and Ye Tao[†,*]

[†]Institute for Microstructural Sciences and [‡]Institute for Chemical Process and Environmental Technology, National Research Council of Canada, 1200 Montreal Road, Ottawa, Ontario K1A 0R6, Canada

ABSTRACT: We report the investigation of the air photostability of benzo[1,2-*b*:4,5-*b*′]dithiophene (BDT) based conjugated polymers using UV−visible spectroscopy, X-ray photoelectron spectroscopy, gel permeation chromatography, and nuclear magnetic resonance spectroscopy. Three low band gap alternating D−A copolymers consisting of 3-fluoro-2-heptylcarbonylthieno[3,4-b]thiophene and alkyl-substituted BDT, alkoxy-substituted BDT, or dithienosilole, respectively, were prepared for investigating their photovoltaic performance and photostability. After only two hours of simultaneous exposure to light and air, the main absorption peak of the polymer films containing BDT units blue-shifted and its intensity dramatically decreased. We demonstrated that the BDT unit underwent dramatic structural change under illumination in air by reacting with the oxygen molecules at the excited state, leading to the disruption of the main-chain conjugation of the polymer. As a result, the color of the alkyl-BDT based polymer film permanently changed from deep blue to light yellow. In contrast, the dithienosilole based polymer was quite stable when treated under the same condition with negligible change in the absorption spectrum.

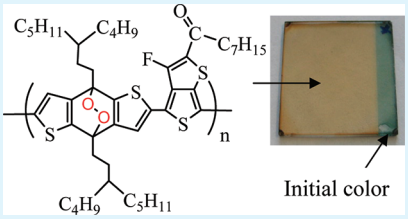

KEYWORDS: *benzodithiophene, low band gap polymers, solar cell, bulk heterojunction, photostability*

INTRODUCTION

Conjugated organic semiconductors including both polymers and small molecules have been intensively studied in the past decade because of their wide variety of applications in organic electronics, such as organic light-emitting diodes,[1] organic field effect transistors (OFET),[2] and organic photovoltaics.[3] In the past few years, the benzo[1,2-*b*:4,5-*b*′]dithiophene (BDT) unit has emerged as a very attractive building block for the construction of conjugated organic semiconductors for applications in OFETs[4] and organic bulk heterojunction (BHJ) solar cells.[3c,d,5] Its large, rigid, and coplanar structure enhances $\pi-\pi$ stacking in the solid state, thus affording a high mobility to the resulting device. To date, polymers based on BDT and thiophene units exhibit a high hole mobility up to 0.25 $cm^2\ V^{-1}\ s^{-1}$.[4c]

Numerous low bandgap p-type polymers incorporating BDT units have been developed for solar cell applications, showing power conversion efficiency (PCE) as high as 7%. Among these polymers, an alternating copolymer (PTB7) of 3-fluorothieno-[3,4-*b*]thiophene-2-carboxylate and benzo[1,2-*b*:4,5-*b*′]-dithiophene shows a PCE of 8.37% by incorporating a thin cathode interface layer with a favorable dipole moment into the device.[5a] Whereas, the PCE of organic solar cells (OSC) is rapidly approaching 10%, the key market-entry criteria, the device stability is still a major concern and is relatively less studied in the literature.[6]

Despite some successful attempts to address the stability issue, such as using inverted organic solar cell structures,[7] air-stable electrode materials, and better encapsulation techniques, the ultimate device lifetime of OSC is still limited by the stability of their active components. Recently, we reported two new alternating alkyl-substituted benzo[1,2-*b*:4,5-*b*′]-dithiophene and ketone-substituted thieno[3,4-*b*]thiophene copolymers with low-lying HOMO energy levels for solar cell applications.[8] We found these two polymers degraded very quickly when exposed to sunlight in air. To investigate the origin of the degradation, we prepared three low bandgap D−A copolymers containing the same electron-withdrawing unit, 3-fluoro-2-heptylcarbonylthieno[3,4-b]thiophene (FTT). The chemical structures of these three polymers are shown in Scheme 1. **P1** and **P2** have been reported in the literature,[8,3d]

Scheme 1. Chemical Structures of Polymers P1-3

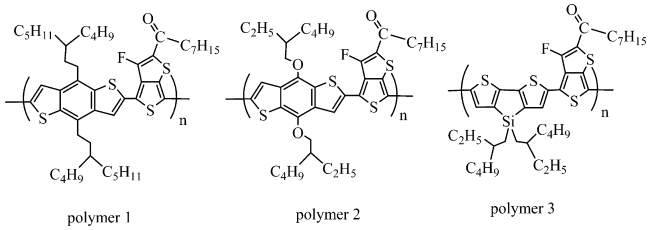

but **P3** is new. We investigated the photovoltaic performance of these three polymers in BHJ solar cells with an active area as large as 1.0 cm^2. The power conversion efficiency achieved from **P1**−**P3** was 3.9, 6.0, and 4.8%, respectively. More importantly, we performed a systematic study on the photostability of these three polymers by UV−vis absorption

Received: February 28, 2012
Accepted: May 2, 2012
Published: May 2, 2012

spectroscopy, X-ray photoelectron spectroscopy (XPS), gel permeation chromatography (GPC) and nuclear magnetic resonance spectroscopy (NMR). We identified that the benzo[1,2-*b*:4,5-*b*′]dithiophene unit was responsible for the photodegradation of the polymers. This unit reacted quickly with the oxygen molecules in the excited state, leading to a disruption of the main-chain conjugation. Moreover, this reaction was not reversible. As a result, the color of the polymer film permanently changed from deep blue to light yellow. This finding is important for the researchers working in the field of organic electronics especially when they design the organic materials for use in the devices which operate in the light.

2. EXPERIMENTAL SECTION

Instrumentation. NMR spectra were recorded on a 400 MHz Varian Unity Inova spectrometer. The photodegraded sample for the NMR measurement was prepared as follows: Polymer **P1** (10 mg) was cast into a film from a chloroform solution in a Petri dish. Then, the film was exposed to sunlight in air. After the film color had completely changed to light yellow, the sample was dissolved in deuterated 1,2-dichlorobenzene for NMR analysis. It was found that the photodegraded polymer was highly soluble in 1,2-dichlorobenzene. Chemical shifts were reported as δ values (ppm) relative to internal tetramethylsilane. Number-average (M_n) molecular weight and polydispersity index (PDI) of the polymers were determined by gel permeation chromatography using Waters Breeze HPLC system with 1525 binary HPLC pump and 2414 differential refractometer. Chlorobenzene was used as eluent and commercial polystyrenes were used as standards. UV−visible absorption spectra were recorded on a Varian Cary 50 UV−vis spectrophotometer. The differential scanning calorimetry (DSC) analysis was performed on a TA Instruments DSC 2920. DSC traces were measured at a scanning rate of 20 °C/min, under a nitrogen flow (50 mL/min). Cyclic voltammetry (CV) measurements were carried out under argon in a three-electrode cell using 0.1 M Bu_4NPF_6 in anhydrous CH_3CN as the supporting electrolyte. The polymers were coated on a platinum-working electrode. The CV curves were recorded referenced to an Ag quasi-reference electrode, which was calibrated using a ferrocene/ferrocenium (Fc/Fc^+) redox couple (4.8 eV below the vacuum level) as an external standard. The $E_{1/2}$ of the Fc/Fc^+ redox couple was found to be 0.40 V versus the Ag quasi-reference electrode. Therefore, the HOMO and LUMO energy levels of the polymers can be estimated using the empirical $E_{HOMO} = -(E_{ox}^{onset} + 4.40)$ eV and $E_{LUMO} = -(E_{red}^{onset} + 4.40)$ eV, respectively, where E_{ox}^{onset} and E_{red}^{onset} are the onset potentials for oxidation and reduction relative to the Ag quasi-reference electrode, respectively. For XPS measurements, the polymer films were spin-coated onto silicon wafer from chlorobenzene solution. The XPS spectra were recorded on a Phi 5500 system, using a monochromatic Al X-ray source with beam energy of 1486 eV and a takeoff angle of 45 degrees.

Materials. All starting materials, unless otherwise specified, were purchased from Aldrich Co. and used without further purification. The tetrahydrofuran used in the reactions was freshly distilled over sodium under argon. Column chromatography was carried out on silica gel (Size 40 - 63 μm, Pore size 60 Å, Silicycle). Monomers 2,6-bis(trimethyltin)-4,8-bis(3-butyloctyl)benzo[1,2-*b*:4,5-*b*′]dithiophene,[8] 2,6-bis(trimethyltin)-4,8-bis(2-ethylhexyloxy)benzo[1,2-*b*:4,5-*b*′]-dithiophene,[5f] 4,4-Bis(2-ethylhexyl)-2,6-bis(trimethyltin)-dithieno[3,2-*b*:2′,3′-*d*]silole,[9] and 1-(3-fluoro-4,6-dibromothieno[3,4-*b*]thiophen-2-yl)octan-1-one[8] were synthesized according to our previously reported procedures. All three polymers **P1**,[8] **P2**[3d] and **P3** were synthesized by Stille coupling reactions in refluxing toluene/DMF (10:1) under Ar using $Pd(PPh_3)_4$ as the catalyst for 42 h. The polymers were purified by Soxhlet extraction with hexanes, dichloromethane, and chloroform.

Polymer **P1**: Yield 70%. M_n = 20.2 kDa and PDI = 1.75. ^{1}H NMR (400 MHz, 1,2-dichlorobenzene-d_4, 140 °C, ppm) δ 7.82 (br, 1H), 7.46 (br, 1H), 3.22 (br, 6H), 2.00−1.35 (m, 44H), 1.25−0.95 (m, 15H).

Polymer **P2**: Yield 95%. M_n = 25.1 kDa and PDI = 1.77. ^{1}H NMR (400 MHz, 1,2-dichlorobenzene-d_4, 50 °C, ppm) δ 7.79 (br, 1H), 7.34 (br, 1H), 4.13 (br, 4H), 3.10 (br, 2H), 2.60−0.8 (m, 43H).

Polymer **P3**: Yield 52%. M_n = 25.7 kDa and PDI = 1.50. ^{1}H NMR (400 MHz, 1,2-dichlorobenzene-d_4, 50 °C, ppm) δ 7.66 (br, 1H), 7.45 (br, 1H), 2.99 (m, 2H), 2.60−0.6 (m, 47H).

Device Fabrication and Characterization. The BHJ solar cells were fabricated on prepatterned ITO coated glass substrates. The sheet resistance and thickness of the ITO are 12 Ω/sq and 150 nm, respectively. The ITO substrates were thoroughly cleaned in detergent and DI water, ultrasonicated in acetone and isopropyl alcohol for 15 min, and dried in an oven at 120 °C. UV-ozone treatment was then performed for 15 min. A 30 nm-thick film of PEDOT:PSS (Baytron P) was spin-cast on top of the ITO substrates and then dried for 15 min at 140 °C. Afterward, an active layer was spin-cast onto the PEDOT:PSS film from chlorobenzene solution of polymer:$PC_{71}BM$ with a weight ratio of 1:1.5 and dried overnight at room temperature in a nitrogen-filled glovebox. The polymer: $PC_{71}BM$ solution with a polymer concentration of 10 mg/mL was prepared three days before deposition and heated at 100 °C for 2 h in a nitrogen-filled glovebox. The spin-coating rate was adjusted between 700 and 1000 rpm to get 100 nm thick active layers. Finally, to complete the solar cell architecture, a bilayer cathode consisting of 100 nm Al on top of 5 nm bathocuproine (BCP) was thermally evaporated through a shadow mask on the active layer to form cells with an active area of 1 cm^2.

The photovoltaic parameters were extracted from the current−voltage (J−V) characteristics measured in air with a Keithley 2400 Digital SourceMeter and the photocurrent was generated under air mass 1.5 global (AM 1.5G) irradiation of 100 mW/cm^2 from a ScienceTech SS 500W solar simulator. The light intensity was adjusted using a calibrated Si photodiode with a KG-5 filter purchased from PV Measurements, Inc. The thicknesses of the polymer films were measured by a Dektak profilometer.

3. RESULTS AND DISCUSSION

Physical Properties. The optical properties of **P1**−**P3** thin films were characterized by UV−vis absorption spectroscopy. As shown in Figure 1, **P1**−**P3** showed absorption maxima at

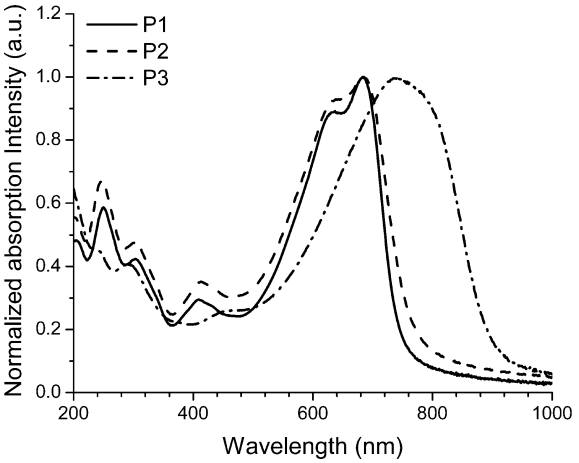

Figure 1. Absorption spectra of polymers **P1**−**P3** in thin films.

683, 685, and 743 nm, respectively. These values match well with the maximum photon flux region in the solar spectrum (~700 nm). The optical bandgaps of polymers **P1**−**P3** calculated from the film absorption edges are 1.65, 1.62, and 1.37 eV, respectively. The bandgap of **P1** is very similar to that of **P2**, which suggests that the replacement of the alkoxy chains on the BDT unit by alkyl chains has very little influence on the

Table 1. Physical Properties of Alternating Copolymers P1−P3

polymers	M_n (KDa)	PDI	T_g (°C)	λ^{abs}_{max} (nm)[a]	E_g (eV) (UV)[a]	E_{HOMO}[b] (eV)	E_{LUMO}[c] (eV)
P1	20.2	1.75	143.7[d]	683	1.65	5.34	3.53
P2	25.1	1.77	189.7	685	1.62	5.22	3.45
P3	25.7	1.50	186.2	743	1.37	4.90	3.37

[a]Measured on the polymer films spin-coated on quartz slides. [b]Estimated from the onset potential of the oxidation wave. [c]Estimated from the onset potential of the reduction wave. [d]P1 has a melting point at 208.5 °C in the first DSC scan.

bandgaps for this class of polymers, as reported in the literature.[3d,8] In contrast, polymer **P3** has a much narrower bandgap. It could be a good candidate for applications in tandem solar cells because of its strong absorption in the near IR region. This suggests that different combinations of electron donor and electron acceptor units can result in totally different optoelectronic properties. DSC analysis showed that polymer **P1** is a crystalline material with a melting point of 208.5 °C during the first DSC scan. However, its second DSC scan revealed a glass transition at 143.7 °C, and a broad melting process above 185 °C. In contrast, both polymers **P2** and **P3** are amorphous materials with a glass transition temperature at 189.7 and 186.2 °C, respectively. The HOMO and LUMO energy levels of **P1**, **P2**, and **P3** were evaluated by CV measurement, based on the onset potentials of the oxidation and reduction waves, respectively. The results are summarized in Table 1. It is interesting to point out that the HOMO energy level of **P1** is 0.12 eV lower than that of **P2**, confirming that the replacement of the alkoxy chains on the BDT unit with less electron-donating alkyl chains can simultaneously lower both the HOMO and LUMO energy levels for this class of polymers. Moreover, **P1** should have a good air stability in the ground state as its HOMO energy level lies below the air oxidation threshold (5.27 eV).[10]

Photovoltaic Performance. Photovoltaic performance of **P1−P3** were investigated in BHJ solar cells, using a device structure of ITO/PEDOT:PSS/Polymer:$PC_{71}BM$ (1:1.5 by weight)/BCP/Al with a device active area of 1.0 cm^2. The use of processing additives, such as DIO, has been proven an effective method to modify and control the nanoscale morphology in polymer solar cells.[11] Therefore, all **P1−P3**-based devices tested in this work were prepared using chlorobenzene/DIO (97/3, v/v) mixture as the solvent. The DIO was added to the solutions right before use. Figure 2 shows the $J-V$ characteristics and external quantum efficiency (EQE) curves of **P1−P3** based BHJ solar cells under simulated AM 1.5G irradiation of 100 mW/cm^2. A significant increase in short-circuit current density (J_{sc}) is clearly observed from **P1** (8.6 mA/cm^2) and **P2** (12.4 mA/cm^2) to **P3** (14.1 mA/cm^2). This increase in J_{sc} is consistent with the increased optical absorption of **P3** at longer wavelengths. However, we have to point out that although **P1** and **P2** have similar bandgaps and absorption spectra, the photocurent obtained from **P2** is much larger. These two polymers have similar hole mobility (~5 × 10^{-4} cm^2 V^{-1} s^{-1}), but **P2** has a much better solubility than **P1**. Therefore, the significant difference in the short circuit currents between **P1** and **P2**-based OSCs might be partly due to the difference in the active layer morphology. In addition, the bulky alkyl chains ($C_{12}H_{25}$) of **P1** may also have some impact on the charge transfer from the polymer to the fullerene derivative. On the other hand, replacing the alkoxy side chains in **P2** by 3-butyloctyl side chains lowers the HOMO energy level of **P1**, leading to an increase in the open-circuit voltage (Voc) from 0.74 V (**P2**) to 0.84 V (**P1**). However, when replacing the BDT unit by the more electron-rich dithienosilole unit in **P3**, the HOMO energy level was greatly raised. As a consequence, the V_{oc} decreased to 0.55 V. The fill factor of **P1−3** based devices is 0.54, 0.65, and 0.62, respectively. The overall EQE-calibrated power conversion efficiency of **P1−3** is 3.9, 6.0, and 4.8%, respectively.

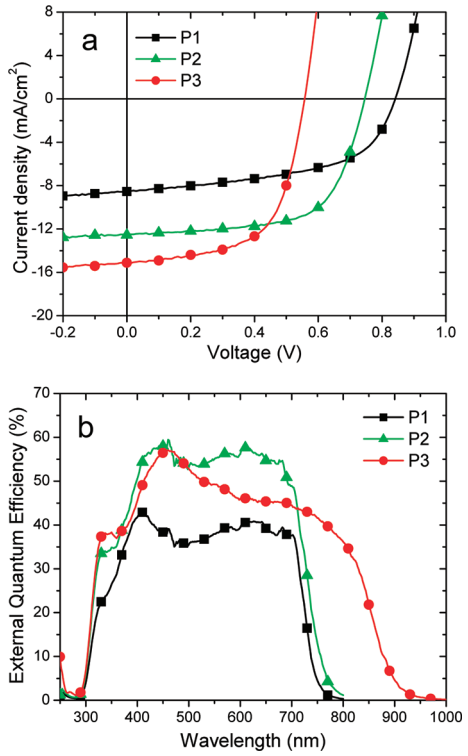

Figure 2. (a) $J-V$ characteristics and (b) EQE curves of **P1−P3**-based BHJ solar cells.

Photostability. To investigate the chemical stability under simultaneous exposure to the simulated sunlight and air, polymer thin films were spin-coated on quartz substrates from **P1**, **P2**, and **P3** chlorobenzene solutions, respectively. The relative humidity of the ambient atmosphere during samples exposure was about 50 to 60%. The absorption spectrum of each film was recorded, before a simultaneous air/light exposure and after 1 min, 30 min, 1 and 2 h of exposure, as shown in Figure 3. The absorption peak of the **P1** film significantly decreased in intensity and blue-shifted after 30 min of exposure to light in air, and completely diminished after 2 h of exposure. Consequently, the film color changed from blue to light yellow (as shown in the inset of the Figure 3), indicating a disruption of the polymer backbone conjugation. Moreover, **P1** completely lost its hole mobility after photodegradation. A less significant decrease in the peak absorption intensity was also observed in the **P2** film, while the absorption of the **P3** film almost remained unchanged after 2 h and even up to 4 h of exposure to light in air under the same conditions. This

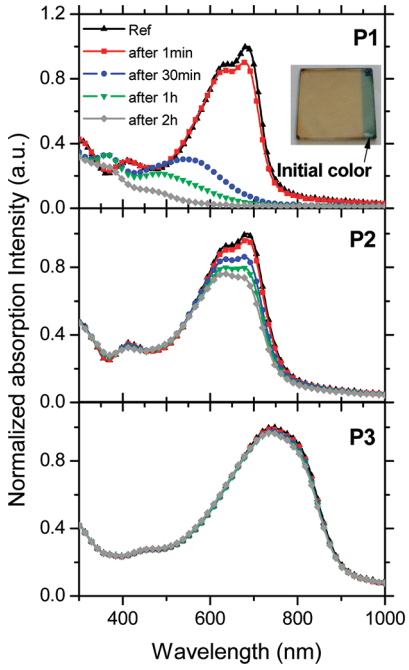

Figure 3. Changes in the absorption spectra of **P1**–**P3** films when exposed to light in air. The inset shows the change in color of **P1** film after 2 h exposure to light in air.

suggests that the chemical instability is related to the BDT unit as **P3** does not contain this unit but both **P1** and **P2** do. In addition, the better stability of **P2** over **P1** also implies that the side chains also affect the polymer stability. It is worth mentioning that **P1** has the deepest HOMO energy level among these three polymers and it is quite stable in the dark. This leads us to conclude that the instability of **P1** and **P2** when exposed simultaneously to light and air is linked to some photochemical reactions occurring at the excited states. Another fact is that the absorption spectra of **P1**–**P3** films have little change when the films are exposed to simulated sunlight in a nitrogen-filled glovebox or have been stored in air in the dark. This means that the instability of the BDT unit is associated with the photochemical reaction of **P1** and **P2** with the oxygen molecules at the excited state.

Contrarily to MDMO-PPV and P3HT,[12] mixing **P1** with fullerene does not improve its photostability. Figure 4 shows the comparison of the absorption spectra of the P1:PC71BM blend (1:2 by weight) film before and after 2 h air/light exposure. The film thickness is about 100 nm. The polymer absorption peak at 683 nm completely vanished after 2 h; consequently, the blend film absorption spectrum matched with the one of $PC_{71}BM$. After the active layers had been exposed to simulated sunlight (100 mW/cm^2) in air for 2 h, the bilayer cathode was evaporated on top of the active layers in order to investigate the change in the photovoltaic performance after photodegradation. As a result, the **P1**-based device showed a very poor performance. The J_{sc} and fill factor dramatically decreased to 38 μA/cm^2 and 0.17, respectively, and the V_{oc} dropped to 0.8 V. In contrast, the photovoltaic performance of the **P3**-based device only slightly decreased after light/air exposure. The device still exhibited a power conversion efficiency of 3.6% with a J_{sc} of 13 mA/cm^2, a fill factor of 0.5, and an unchanged Voc of 0.55 V.

Investigation on the Degradation Mechanism. We carried out XPS measurements on the polymers films before

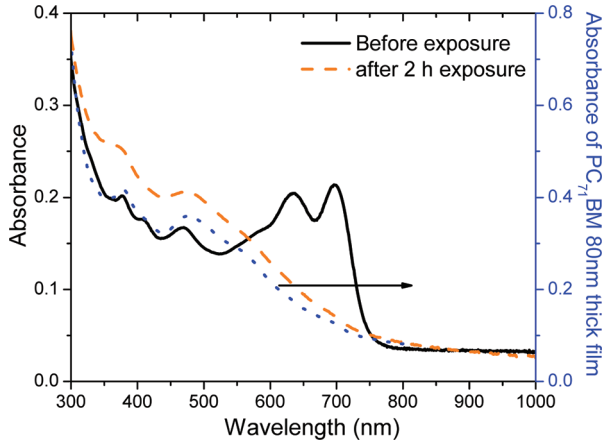

Figure 4. Comparison of absorption spectra of P1:$PC_{71}BM$ blend film before and after light exposure in air and of an 80 nm thick $PC_{71}BM$ film.

and after exposing the samples to sunlight in air. The atomic content of O in the near surface region of the thin films increased from 2 to 11.8% after 2 h exposure to light in air. Figure 5 shows the dramatic increase of O content. Moreover,

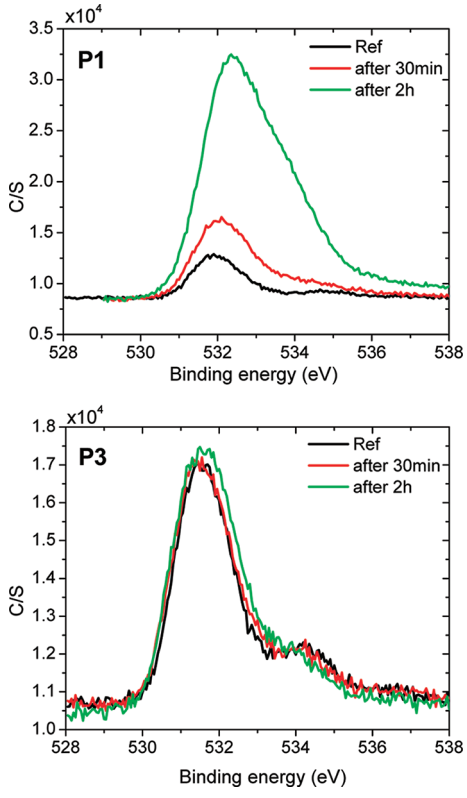

Figure 5. Comparison of XPS oxygen content in **P1** and **P3** film surfaces before and after 30 min and 2 h exposure to light in air.

this increase in the oxygen content is not reversible, and the oxygen cannot be removed by heating or pumping in the vacuum. This suggests that the oxygen atoms are chemically attached to the polymer. In contrast, the oxygen content of **P3** shows no change after the film was exposed to air and light for 2 h, which is consistent with the excellent stability of **P3** against the photo oxidation.

GPC analysis on the photodegraded **P1** sample revealed that the degradation process is even more complicated. The photodegraded polymer was highly soluble in organic solvetns, such as chlorobenzene and chloroform, and had a better solubility than the pristine polymer, indicating that no cross-linking reaction occurred during photodegradation. In contrast, the polymer backbone is also cleaved by the photo oxidation process, leading to a decrease of the molecular weight from ~20 to ~6 KDa, as shown in Figure 6. Another strong evidence for the break in the polymer backbone is that the polymer lost its hole mobility after photodegradation.

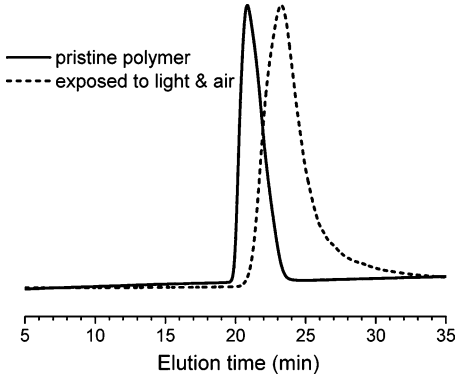

Figure 6. Decrease in the molecular weight of **P1** after photooxidation.

NMR analysis also shed light on the structural change of polymer **P1** upon photooxidation. As can be seen from Figure 7, **P1** has 6 protons at ~3.22 ppm, corresponding to the two

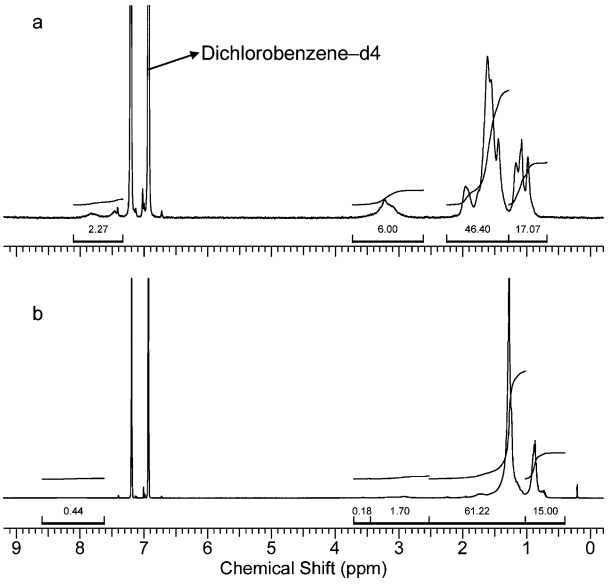

Figure 7. Change in the proton NMR spectra of **P1** (a) before and (b) after photodegradation.

$-CH_2-$ groups attached to the C4 and C8 positions of the BDT unit and the $-CH_2-$ group adjacent to the carbonyl functional group on the FTT unit. After photooxidation, the total proton number in the region from 3.6 to 2.6 ppm decreased to 2, and the two aromatic protons also almost disappeared. These results indicate that the BDT unit underwent dramatic structural change upon photooxidation. It is well-known that anthracene is able to react with singlet O_2 to form the corresponding 9,10-endoperoxide derivative.[13] We believe that the BDT unit underwent the same reaction during photooxidation, leading to the disruption of the backbone conjugation. Singlet O_2 may be generated by photosensitization from the excited state of **P1**. However, it is not yet clear why **P2** is relatively more stable than **P1**. It seems that the alkoxy substituent on the BDT unit in **P2** can retard this photo-oxidation process. The reason is under investigation. In addition, the BDT endoperoxide intermediate formed during photooxidation was not stable and can further decompose, leading to the cleavage of the polymer backbone, as confirmed by the GPC analysis.

4. CONCLUSIONS

In summary, we have prepared three low bandgap alternating copolymers containing a common electron-withdrawing unit, 3-fluoro-2-heptylcarbonylthieno[3,4-b]thiophene, for the investigation of their photostability. We have demonstrated that the different combinations of electron donor and electron acceptor units have a huge impact on the physical and optoelectronic properties of the resulting polymers. Even for the same D−A combination, the side chain substituents also greatly affect the solubility, energy levels and stability of the polymers. More importantly, through a systematic study we have proven that the widely used benzo[1,2-*b*:4,5-*b*′]dithiophene (BDT) unit can cause potential stability issues because it can react quickly with oxygen in the excited state, causing main-chain conjugation disruption and losing its hole mobility. The finding in this work also suggests that a deep HOMO energy level (below 5.27 eV) does not guarantee a good stability against photooxidation.

AUTHOR INFORMATION

Corresponding Author

*E-mail: jianping.lu@nrc-cnrc.gc.ca (J.L.); ye.tao@nrc-cnrc.gc.ca (Y.T.).

Notes

The authors declare no competing financial interest.

ACKNOWLEDGMENTS

The authors thank Mr. Oltion Kodra for XPS measurements and Ms. Raluca Movileanu, Mr. Eric Estwick and Mr. Hiroshi Fukutani for their technical support. This project was supported by the Sustainable Development Technology Canada (SDTC).

REFERENCES

(1) (a) Burroughes, J. H.; Bradley, D. D. C.; brown, A. R.; Marks, R. N.; Mackay, K.; Friend, R. H.; Burn, P. L.; Holmes, A. B. *Nature* **1990**, *347*, 539−541. (b) Friend, R. H.; Gymer, R. W.; Holmes, A. B.; Burroughes, J. H.; Marks, R. N.; Taliani, C.; Bradley, D. D. C.; Dos Santo, D. A.; Brédas, J. L.; Lögdlund, M.; Salaneck, W. R. *Nature* **1999**, *397*, 121−128. (C) Kraft, A.; Grimsdale, A. C.; Holmes, A. B. *Angew. Chem., Int. Ed.* **1998**, *37*, 402−428.

(2) (a) Garnier, F.; Hajlaoui, R.; Yassar, A.; Srivastava, P. *Science* **1994**, *265*, 1684−1686. (b) Bao, Z. *Adv. Mater.* **2000**, *12*, 227−230. (c) Sirringhaus, H.; Kawase, T.; Friend, R. H.; Shimoda, T.; Inbasekaran, M.; Wu, W.; Woo, E. P. *Science* **2000**, *290*, 2123−2126. (d) Minemawari, H.; Yamada, T.; Matsui, H.; Tsutsumi, J.; Haas, S.; Chiba, R.; Kumai, R.; Hasegawa, T. *Nature* **2011**, *475*, 364−367. (e) Tsao, H. N.; Cho, D. M.; Park, I.; Hansen, M. R.; Mavrinskiy, A.; Yoon, D. Y.; Graf, R.; Pisula, W.; Spiess, H.; Müllen, K. *J. Am. Chem. Soc.* **2011**, *133*, 2605−2612.

(3) (a) Yu, G.; Gao, J.; Hummelen, J. C.; Wudl, F.; Heeger, A. J. *Science* **1995**, *270*, 1789−1791. (b) Peet, J.; Kim, J. Y.; Coates, N. E.;

Ma, W. L.; Moses, D.; Heeger, A. J.; Bazan, G. C. *Nat. Mater.* **2007**, *6*, 497−500. (c) Liang, Y.; Xu, Z.; Xia, J.; Tsai, S.; Wu, Y.; Li, G.; Ray, C.; Yu, L. *Adv. Mater.* **2010**, *22*, E135−E138. (d) Chen, H. Y.; Hou, J.; Zhang, S.; Liang, Y.; Yang, G.; Yang, Y.; Yu, L.; Wu, Y.; Li, G. *Nat. Photon.* **2009**, *3*, 649−653. (e) Chu, T.-Y.; Lu, J.; Beaupré, S.; Zhang, Y.; Pouliot, J.-R.; Wakim, S.; Zhou, J.; Leclerc, M.; Li, Z.; Ding, J.; Tao, Y. *J. Am. Chem. Soc.* **2011**, *133*, 4250−4253.

(4) (a) Mamada, M.; Kumaki, D.; Nishida, J.-I.; Tokito, S.; Yamashita, Y. *ACS applied materials interfaces* **2010**, *2*, 1303−1307. (b) Leenen, M. A.M.; Cucinotta, F.; Pisula, W.; Steiger, J.; Anselmann, R.; Thiem, H.; De Cola, L. *Polymer* **2010**, *51*, 3099−3107. (c) Pan, H.; Li, Y.; Wu, Y.; Liu, P.; Ong, B. S.; Zhu, S.; Xu, G. *J. Am. Chem. Soc.* **2007**, *129*, 4112−4113.

(5) (a) He, Z.; Zhong, C.; Huang, X.; Wong, W.-Y.; Wu, H.; Chen, L.; Su, S.; Cao, Y. *Adv. Mater.* **2011**, *23*, 4636−4643. (b) Price, S. C.; Stuart, A. C.; Yang, L.; Zhou, H.; You, W. *J. Am. Chem. Soc.* **2011**, *133*, 4625−4631. (c) Nie, W.; MacNeill, C. M.; Li, Y.; Noftle, R. E.; Carroll, D. L.; Coffin, R. C. *Macromol. Rapid Commun.* **2011**, *32*, 1163−1168. (d) Zhang, Y.; Li, Z.; Wakim, S.; Alem, S.; Tsang, S.-W.; Lu, J.; Ding, J.; Tao, Y. *Org. Electron.* **2011**, *12*, 1211−1215. (e) Hou, J.; Park, M.-H.; Zhang, S.; Yao, Y.; Chen, L.-M.; Li, J.-H.; Yang, Y. *Macromolecules* **2008**, *41*, 6012−6018. (f) Liang, Y.; Feng, D.; Wu, Y.; Tsai, S.; Li, G.; Ray, C.; Yu, L. *J. Am. Chem. Soc.* **2009**, *131*, 7792−7799.

(6) (a) Jørgensen, M.; Norrman, K.; Gevorgyan, S. A.; Tromholt, T.; Andreasen, B; Krebs, F. C. *Adv. Mater.* **2012**, *24*, 580−612. (b) Manceau, M.; Bundgaard, E.; Carlé, J. E.; Hagemann, O.; Helgesen, M.; Søndergaard, R.; Jørgensen, M.; Krebs, F. C. *J. Mater. Chem.* **2011**, *21*, 4132−4141. (c) Helgesen, M.; Madsen, M. V.; Andreasen, B.; Tromholt, T.; Andreasen, J. W.; Krebs, F. C. *Polym. Chem.* **2011**, *2*, 2536−2542. (d) Helgesen, M.; Sørensen, T. J.; Manceau, M.; Krebs, F. C. *Polym. Chem.* **2011**, *2*, 1355−1361. (e) Tromholt, T.; Manceau, M.; Helgesen, M.; Carlé, J. E.; Krebs, F. C. *Sol. Energy Mater. Sol. Cells* **2011**, *95*, 1308−1314.

(7) (a) White, M. S.; Olson, D. C.; Shaheen, S. E.; Kopidakis, N.; Ginley, D. S. *Appl. Phys. Lett.* **2006**, *89*, 143517. (b) Hau, S. K.; Yip, H. L.; Baek, N. S.; Zou, J.; O'Malley, K.; Jen, A. K. Y. *Appl. Phys. Lett.* **2008**, *92*, 253301. (c) Lloyd, M. T.; Olson, D. C.; Lu, P.; Fang, E.; Moore, D. L.; White, M. S.; Reese, M. O.; Ginley, D. S.; Hsu, J. W. P. *J. Mater. Chem.* **2009**, *19*, 7638−7642. (d) Chu, T.-Y.; Tsang, S.-W.; Zhou, J.; Verly, P. G.; Lu, J.; Beaupré, S.; Leclerc, M.; Tao, Y. *Sol. Energy Mater. Sol. Cells* **2012**, *96*, 155−159.

(8) Wakim, S.; Alem, S.; Li, Z.; Zhang, Y.; Tse, S.-C.; Lu, J.; Ding, J.; Tao, Y. *J. Mater. Chem.* **2011**, *21*, 10920−10928.

(9) (a) Liao, L.; Dai, L.; Smith, A.; Durstock, M.; Lu, J.; Ding, J.; Tao, Y. *Macromolecules* **2007**, *40*, 9406−9412. (b) Hou, J.; Chen, H.; Zhang, S.; Li, G.; Yang, Y. *J. Am. Chem. Soc.* **2008**, *130*, 16144−16145.

(10) de Leeuw, D. M.; Simenon, M. M. J.; Brown, A. R.; Einhard, R. E. F. *Synth. Met.* **1997**, *87*, 53−59.

(11) Lee, J. K.; Ma, W. L.; Brabec, C. J.; Yuen, J.; Moon, J. S.; Kim, J. Y.; Lee, K.; Bazan, G. C.; Heeger, A. J. *J. Am. Chem. Soc.* **2008**, *130*, 3619−3623.

(12) (a) O. Reese, M.; Nardes, A. M.; Rupert, B. L.; Larsen, R. E.; Olson, D. C.; Lloyd, M. T.; Shaheen, S. E.; Ginley, D. S.; Rumbles, G.; Kopidakis, N. *Adv. Funct. Mater.* **2011**, *20*, 3476−3483. (b) Neugebauer, H.; Brabec, C.; Hummelen, J. C.; Sariciftci, N. S. *Sol. Energy Mater. Sol. Cells* **2000**, *61*, 35−42.

(13) (a) Wasserman, H. H.; Scheffer, J. R.; Cooper, J. L. *J. Am. Chem. Soc.* **1972**, *94*, 4991−4996. (b) Massari, J.; Tokikawa, R.; Medinas, D. B.; Angeli, J. P. F.; Mascio, P. D.; Assuncao, N. A.; Bechara, E. J. H. *J. Am. Chem. Soc.* **2011**, *133*, 20761−20768.